Further analysis of energy-based indentation relationship among Young's modulus, nominal hardness, and indentation work

Dejun Ma[a)]
Department of Mechanical Engineering, The Academy of Armored Forces Engineering, Beijing 100072, People's Republic of China

Chung Wo Ong[b)]
Department of Applied Physics and Materials Research Center, The Hong Kong Polytechnic University, Hung Hom, Kowloon, Hong Kong, People's Republic of China

(Received 9 December 2009; accepted 19 February 2010)

In our previous study, we modeled the indentation performed on an elastic–plastic solid with a rigid conical indenter by using finite element analysis, and established a relationship between a nominal hardness/reduced Young's modulus (H_n/E_r) and unloading work/total indentation work (W_e/W_t). The elasticity of the indenter was absorbed in $E_r \equiv 1/[(1-\nu^2)/E + (1-\nu_i^2)/E_i]$, where E_i and ν_i are the Young's modulus and Poisson's ratio of the indenter, and E and ν are those of the indented material. However, recalculation by directly introducing the elasticity of the indenter show that the use of E_r alone cannot accurately reflect the combined elastic effect of the indenter and indented material, but the ratio $\eta = [E/(1-\nu^2)]/[E_i/(1-\nu_i^2)]$ would influence the H_n/E_r–W_e/W_t relationship. Thereby, we replaced E_r with a combined Young's modulus $E_c \equiv 1/[(1-\nu^2)/E + 1.32(1-\nu_i^2)/E_i] = E_r/[1 + 0.32\eta/(1+\eta)]$, and found that the approximate H_n/E_c–W_e/W_t relationship is almost independent of selected η values over 0–0.3834, which can be used to give good estimates of E as verified by experimental results.

I. INTRODUCTION

Instrumented indentation tests for measuring mechanical properties of materials on small scales have been widely used for more than two decades,[1–3] and other than hardness, Young's modulus is an important material property determinable with this technique. Using the well-known relationship among reduced Young's modulus, initial unloading stiffness and contact area, Oliver and Pharr[4–6] developed a classic method for Young's modulus measurement. However, this method is not always accurate enough. For example, when the indented material exhibits little work hardening, pronounced piling up occurs around an indent, causing difficulty in estimating the contact area. Cheng and Cheng[7,8] proposed an alternative method. They established an approximate relationship among reduced Young's modulus, real hardness and indentation work, and combined Oliver and Pharr's relationship to estimate Young's modulus. This method avoids indirect determination of contact depth as in Oliver and Pharr's method and subsequent error. However, the square of the stiffness evaluated at the initial unloading process appears in the formulation, which is found to be sensitive to the condition of the indentation test and is normally fluctuating at low loads. This greatly affects the applicability of the method.

In our recent studies,[9,10] we developed a new energy-based method for determining Young's modulus of a material. In this method, finite element analysis (FEA) was performed to simulate indentation made on an elastic–plastic solid with a rigid indenter. The elastic effect of an indenter used in a real experiment is absorbed by using a reduced Young's modulus, $E_r \equiv 1/(1-\nu^2)/E + (1-\nu_i^2)/E_i$, where E and ν are the Young's modulus and Poisson's ratio of the indented material; and E_i and ν_i are those of the indenter. An approximate functional relationship between the ratio of nominal hardness/reduced Young's modulus (H_n/E_r) and the ratio of the unloading work/total work of indentation (W_e/W_t) was established, where $H_n \equiv P_m/A(h_m)$ with P_m being the maximum load and $A(h_m)$ the cross-sectional area evaluated at the maximum indentation depth h_m. Note that H_n is different from the real hardness H determined with the area evaluated at the maximum contact depth. The greatest advantage of this method is that H_n can be determined from the primary load and displacement data; and W_e and W_t are in fact the areas under the unloading and loading curves. Thus, one avoids the need of indirectly estimated quantities like the contact depth, and some experimental parameters, which is sensitive to the condition of measurement, such as the initial unloading stiffness used in

Address all correspondence to these authors.
[a)]e-mail: dejunma@yahoo.com
[b)]e-mail: apacwong@inet.polyu.edu.hk
DOI: 10.1557/JMR.2010.0137

Cheng and Cheng's method. The value of E derived from the method is therefore more exact.

In this work, we report further modification of our energy-based method by directly introducing the elasticity of a conical indenter into the FEA model. In particular, the role of E_r in the H_n/E_r–W_e/W_t relationship is replaced by a newly defined combined Young's modulus $E_c \equiv 1/[(1 - \nu^2)/E + 1.32(1 - \nu_i^2)/E_i]$. A functional H_n/E_c–W_e/W_t relationship was established, from which a good estimate of E was achieved as verified by experimental results.

II. NUMERICAL ANALYSES OF SHARP INDENTATION

Within the framework of continuum mechanics, we considered an elastic conical indenter indenting normally into a homogeneous elastic–plastic solid. The half angle of the conical indenter is specified to be 70.3° to approximate the most commonly used Berkovich indenter geometry. The rationale of employing such a setting is based on the fact that the computed load–displacement responses produced by using a real Berkovich tip is found to be virtually identical to that produced by a conical tip having the same area-to-depth ratio.[11,12] We further assumed that the indented material is an isotropic and rate-independent solid, and obeys Von Mises yield criterion and pure isotropic hardening rule. The uniaxial stress–strain relation is a combination of linear elasticity and Hollomon's power law hardening:

$$\sigma = \begin{cases} E\varepsilon, \varepsilon \leqslant \varepsilon_y \\ \sigma_y(\varepsilon/\varepsilon_y)^n, \ \varepsilon > \varepsilon_y \end{cases} \quad , \tag{1}$$

where σ and ε are the true stress and true strain, and σ_y and $\varepsilon_y = \sigma_y/E$ the yield stress and yield strain. If we assume that the indenter is elastic, and interface between the indenter and the indented material is frictionless, the nominal hardness H_n and the work ratio W_e/W_t, regarded as the indentation responses in the analysis, should be functions of the elastoplastic properties (E, ν, σ_y, n) of the tested material, the elastic properties (E_i, ν_i) of the indenter, and the maximum indentation depth (h_m). The correlations between these quantities are expressed implicitly as

$$H_n = f_{H1}(E, \nu, \sigma_y, n, E_i, \nu_i, h_m) \quad , \tag{2}$$

$$W_e/W_t = f_{W1}(E, \nu, \sigma_y, n, E_i, \nu_i, h_m) \quad . \tag{3}$$

According to Dao et al.[11] and Fischer-Cripps,[13] these two functions may be simplified by introducing E_r to combine the overall elasticity effects of the indenter and the indented material, such that Eqs. (2) and (3) can be expressed as

$$H_n = f_{H2}(\sigma_y, n, E_r, h_m) \quad , \tag{4}$$

$$W_e/W_t = f_{W2}(\sigma_y, n, E_r, h_m) \quad . \tag{5}$$

Applying Π theorem of dimensional analysis, functions (4) and (5) can be rewritten in the following dimensionless forms:

$$H_n/E_r = f_{H3}(\sigma_y/E_r, n) \quad , \tag{6}$$

$$W_e/W_t = f_{W3}(\sigma_y/E_r, n) \quad . \tag{7}$$

Considering that σ_y/E_r in Eq. (7) can be expressed in terms of W_e/W_t and n, it can be expressed alternatively as

$$\sigma_y/E_r = f_{W3}^{-1}(W_e/W_t, n) \quad . \tag{8}$$

By substituting Eq. (8) into Eq. (6) to remove σ_y/E_r, the expression of H_n/E_r becomes

$$H_n/E_r = f_{H3}[f_{W3}^{-1}(W_e/W_t, n), n] = f_{HW}(W_e/W_t, n) \quad . \tag{9}$$

To obtain an explicit result, a commercial finite element code ABAQUS[14] capable of handling large deformation analysis was used to simulate the conical indentation process. In the calculations, σ_y was varied to cover a broad range of 0.0005∼160,000 MPa. The n was assigned to have the values of 0, 0.15, 0.3, and 0.45 in sequence. E, ν, E_i, and ν_i were varied in such a way that the Young's modulus ratio $\eta \equiv [E/(1 - \nu^2)]/[E_i/(1 - \nu_i^2)]$ was equal to $[70/(1 - 0.3^2)]/[\infty] = 0$, $[70/(1 - 0.3^2)]/[1141/(1 - 0.07^2)] = 0.0671$, $[200/(1 - 0.3^2)]/[1141/(1 - 0.07^2)] = 0.1917$, and $[400/(1 - 0.3^2)]/[1141/(1 - 0.07^2)] = 0.3834$ successively. In an FEA, four-node axisymmetric elements were used. The size of the elements was made to be small enough for the number of nodes at the contact region to be more than 30. Figure 1 illustrates the model used, where the meshing around the contact region is much finer for ensuring the accuracy of the simulation. The radius of the cross-sectional area of the indenter at h_m is below 1/40 of the

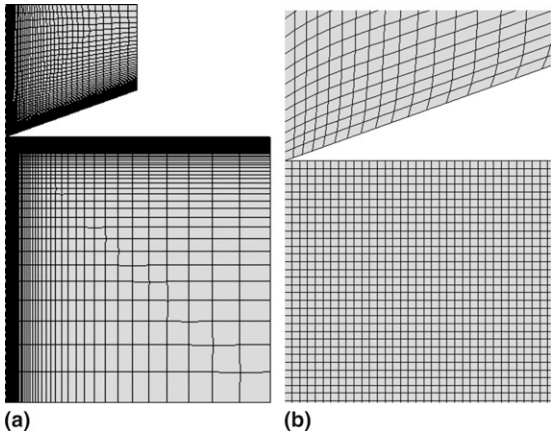

FIG. 1. Finite elements mesh design for a conical indenter and an indented solid. (a) Overall view and (b) details around the contact region.

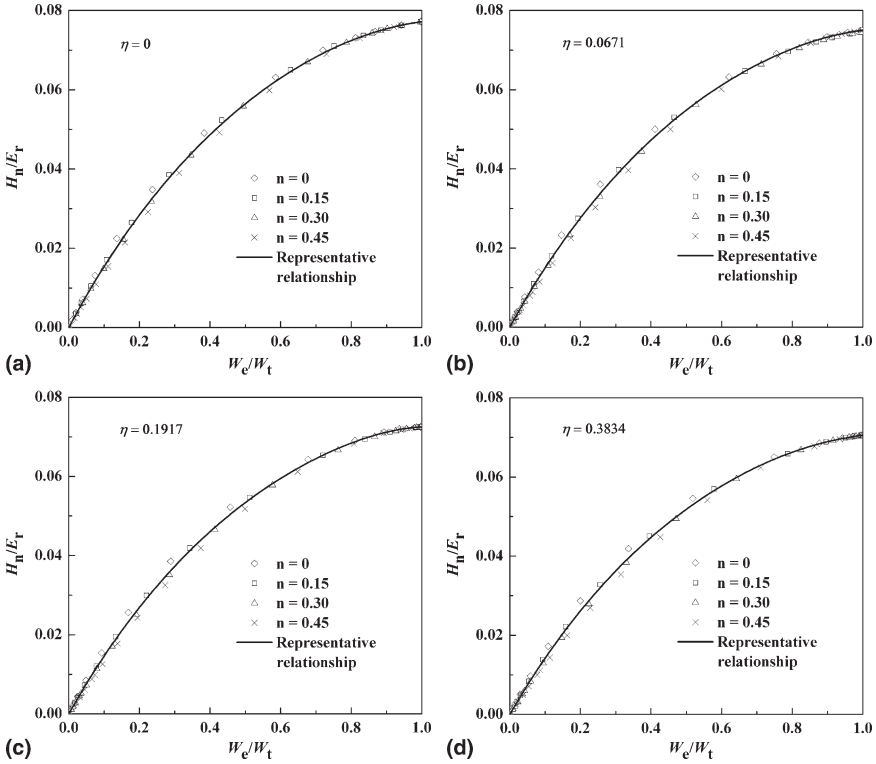

FIG. 2. (a)–(d) Plots of H_n/E_r versus W_e/W_t with different values of n for $\eta = 0$, 0.0671, 0.1917, and 0.3834.

dimension of the indented material model. The indented material and indenter were meshed into 8100 and 2500 elements, respectively. The design of the model passed a sensitivity test, which indicates that the change of the calculated results was less than 0.5% even when the mesh size was reduced by 50%, or the model size was doubled in both the radial and vertical directions.

Figures 2(a)–2(d) show the plots of H_n/E_r versus W_e/W_t corresponding to four $\eta = 0$, 0.15, 0.3, and 0.45, respectively, with each containing data of different values of n. It is evident that the data points in each figure fall in a narrow band bounded between the curves of $n = 0$ and 0.45. Therefore, H_n/E_r and W_e/W_t can be regarded to have a functional relationship. Such a relationship is describable with a sixth-order polynomial, which is referred to as the representative relationship afterwards. The four representative relationships associated with the four values of η are plotted in Figs. 2(a)–2(d), respectively. Obviously, if E_r is effective in reflecting the combined elastic effect of the indenter and indented material, all of the four curves should merge together disregarding their values of η. However, their plots shown in Fig. 3 show some degree of inconsistency, leading one to infer that the variation of η would indeed alter the functional form of H_n/E_r against W_e/W_t. As such, the H_n/E_r–W_e/W_t relationship may not be the best for the use of determining the Young's modulus of an indented

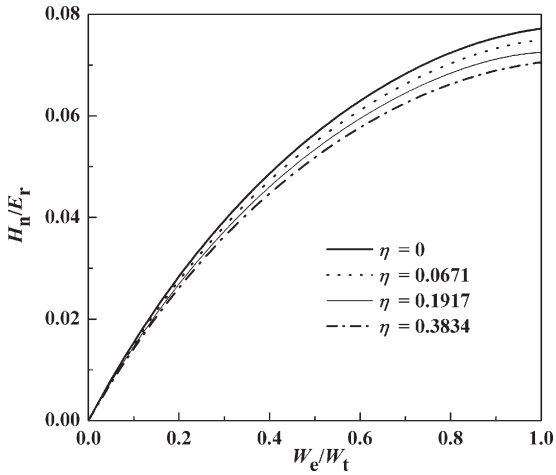

FIG. 3. Representative H_n/E_r–W_e/W_t relationships for $\eta = 0$, 0.0671, 0.1917, and 0.3834.

substance with the energy-based method. A natural thought is to develop a new closed-form relationship among Young's modulus, nominal hardness, and indentation work. In this work, we propose to use a combined Young's modulus $E_c \equiv 1/[(1 - \nu^2)/E + 1.32(1 - \nu_i^2)/E_i] = E_r/[1 + 0.32\eta/(1 + \eta)]$ to replace E_r. The resulted H_n/E_c values are plotted in Fig. 4 against W_e/W_t. The plot indicates an effective one-to-one correspondence between H_n/E_c and W_e/W_t disregarding the value

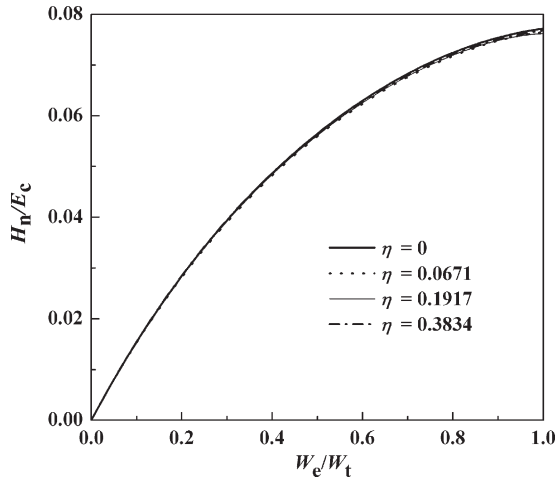

FIG. 4. Representative H_n/E_c–W_e/W_t relationships for $\eta = 0$, 0.0671, 0.1917, and 0.3834.

of η. The data points can be fitted to a sixth-order polynomial:

$$H_n/E_c = \sum_{i=1}^{6} a_i (W_e/W_t)^i \quad , \qquad (10)$$

where the coefficients are determined as $a_1 = 0.16716$, $a_2 = -0.13875$, $a_3 = 0.06215$, $a_4 = 0.01568$, $a_5 = -0.04784$, and $a_6 = 0.01878$.

Successful establishment of Eq. (10) forms the basis for determining Young's modulus by means of microindentation tests, when the influence of the tip bluntness of a real Berkovich indenter is negligible.

III. METHOD FOR DETERMINING YOUNG'S MODULUS BASED ON MICROINDENTATION TESTS

On the basis of the newly revealed relationship between H_n/E_c and W_e/W_t described by Eq. (10), the detailed procedures for determining Young's modulus by applying instrumented microindentation tests are given as follows:

(i) Generate loading and unloading curves by performing microindentation on a tested material with a Berkovich indenter. P_m and h_m are directly measured to give the value of $H_n \equiv P_m/A(h_m)$. When $h_m \geqslant 3$ μm, the value of $A(h_m)$ is equal to 24.5 h_m^2. When 1 μm $\leqslant h_m \leqslant$ 3 μm, $A(h_m)$ is proposed to be determined according to the calibrated area function generated from the method proposed by Oliver and Pharr.[4,6]

(ii) Calculate the indentation unloading work and the total work by integrating the areas under the unloading and loading curves, respectively, and then determine the work ratio W_e/W_t.

(iii) Determine the combined Young's modulus $E_c = H_n/\left[\sum_{i=1}^{6} a_i (W_e/W_t)^i\right]$, and then the Young's modulus of the tested material by using the expression $E = (1 - \nu^2)/[1/E_c - 1.32(1 - \nu_i^2)/E_i]$, provided that the values of E_i, ν_i, and ν are all known.

The stability for the determination of E_c can be examined by investigating the sensitivity of E_c with respect to perturbations of H_n and W_e/W_t. The dispersion of E_c calculated from the formula $E_c = H_n/\left[\sum_{i=1}^{6} a_i (W_e/W_t)^i\right]$ by varying W_e/W_t with ±5% around a centered value selected arbitrarily from a range of 0.01∼1 is less than ± 5.2%, while the same change of H_n would lead to the same variation of E_c. It is thus concluded that E_c exhibits a rather good stability over small perturbations of H_n and W_e/W_t.

The error of this method in determining E_c is the same as that of our previous method in determining E_r for an ideal Berkovich indenter model analyzed in our previously published work.[10] It has been found that the errors always decrease with the work ratio W_e/W_t increasing, and the maximum error is ±13.3% when W_e/W_t approaches zero. From the engineering point of view, such a level of accuracy in the measurement of Young's modulus can meet the requirements of most applications. Further improvement of the accuracy should turn to the use of multiple sharp indentation tests, and the works of Lan and Venkatesh[15] and Liu et al.,[16] provided a good guideline on how to extract the elastic and plastic properties of materials with high accuracy and reduced sensitivity.

IV. EXPERIMENTAL EXAMPLES

We first referred to some published data of microindentation tests for two aluminum alloys 6061-T6511 and 7075-T651[11] to examine the effectiveness of the method. The Young's moduli extracted from uniaxial tension tests for these two materials are 66.8 and 70.1 GPa, respectively, and their Poisson's ratio are both 0.33. The results of the indentation tests are summarized in Table I, in which h_m is evaluated from the equation $h_m = (P_m/C)^{1/2}$, with C being the loading curvature, and the nominal hardness H_n is calculated by using the expression $H_n = P_m/(24.5h_m^2)$. In addition, the results of Young's modulus $E_{O\&P}$ determined by the Oliver and Pharr method are also shown in Table I. It is obvious that for these two materials with small strain-hardening exponents of 0.08 and 0.122, the currently proposed method appears to be more effective than the traditional one. Thus, it is further believed that the relatively low strain-hardening exponent would cause piling up, which is supposed to be the main reason responsible for the lower accuracy in estimating the Young's modulus of the material by using Oliver and Pharr's method.

In addition, a commercial Nano Indenter XP (MTS Systems Corp., Knoxville, TN) equipped with a Berkovich indenter was used to perform microindentation tests on three materials, i.e., aluminum single crystal, GCr15

TABLE I. The values of E and $E_{O\&P}$ for two aluminum alloys determined from the present method and Oliver & Pharr method.

For Al 6061-T6511								
Test no.	h_m (μm)	S_u (N/mm)	H_n (GPa)	W_e/W_t	E (GPa)	(E-66.8)/E (%)	$E_{O\&P}$ (GPa)	($E_{O\&P}$-66.8)/ $E_{O\&P}$ (%)
1	10.46	4768	1.118	0.098	72.1	7.4	79.3	15.8
2	10.31	4800	1.151	0.095	76.8	13.0	81.2	17.7
3	10.50	4794	1.110	0.096	73.0	8.5	79.5	15.9
4	10.48	4671	1.114	0.111	63.5	−5.3	77.5	13.8
5	10.54	4762	1.102	0.111	62.7	−6.5	78.6	15.0
6	10.43	4491	1.127	0.109	65.4	−2.2	74.9	10.9
Average					68.9	3.0	78.5	14.9
For Al 7075-T651								
Test no.	h_m (μm)	S_u (N/mm)	H_n (GPa)	W_e/W_t	E (GPa)	(E-70.1)/E (%)	$E_{O\&P}$ (GPa)	($E_{O\&P}$-70.1)/ $E_{O\&P}$ (%)
1	8.45	3665	1.714	0.167	68.3	−2.6	77.6	9.7
2	8.56	3658	1.669	0.162	68.3	−2.6	76.3	8.1
3	8.42	3654	1.727	0.168	68.4	−2.4	77.7	9.8
4	8.34	3744	1.759	0.164	71.5	1.9	80.5	12.9
5	8.30	3789	1.776	0.161	73.5	4.6	81.9	14.4
6	8.20	3706	1.820	0.169	72.1	2.8	81.3	13.8
Average					70.3	0.3	79.2	11.5

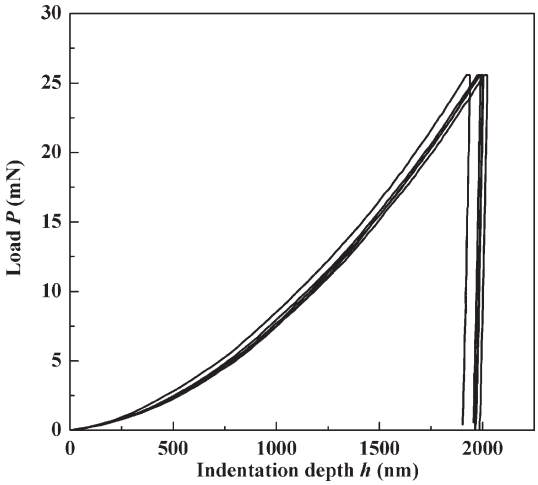

FIG. 5. Load–displacement curves of five repetitive tests performed on aluminum single crystal.

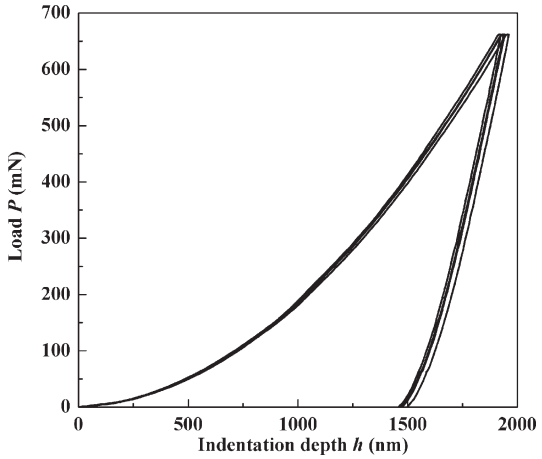

FIG. 6. Load–displacement curves of five repetitive tests performed on GCr15 bearing steel.

bearing steel, and fused silica, where the aluminum single crystal and fused silica are standard samples provided by MTS. Their reference Young's modulus values as claimed by MTS are 70.4 and 72 GPa, respectively. The reference value for GCr15 bearing steel is determined to be 204 GPa by applying standard ultrasonic measurement. The area function $A(h)$ of the indenter was calibrated as $A(h) = 24.4974h^2 + 424.149h + 28211.4h^{1/2} - 69751.1h^{1/4} - 46333.3h^{1/8} - 7055.7h^{1/16} + 20987.7h^{1/32} + 37312.2h^{1/64} + 46075.9h^{1/128}$. An experiment was repeated five times to obtain five sets of load–displacement curves, as shown in Figs. 5–7. The Poisson's ratio ν of aluminum single crystal, GCr15 bearing steel, and fused silica were assigned to be 0.347, 0.29, and 0.17, respectively. By applying the proposed method, the Young's modulus E of the three tested materials were determined. The results

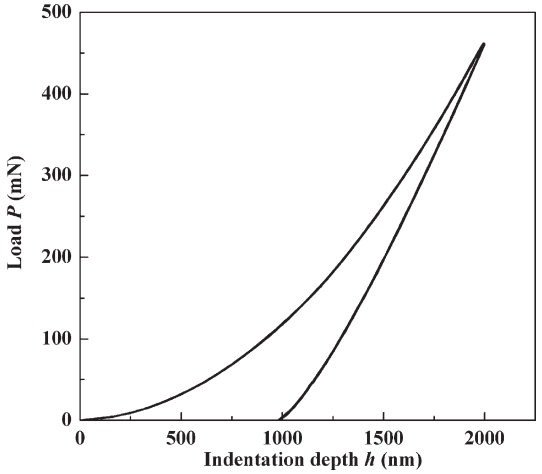

FIG. 7. Load–displacement curves of five repetitive tests performed on fused silica.

TABLE II. The values of E for aluminum single crystal, GCr15 bearing steel, and fused silica determined from the present method.

For aluminum single crystal					
Test no.	h_m (μm)	H_n (GPa)	W_e/W_t	E (GPa)	(E-70.4)/E (%)
1	2.001	0.256	0.0262	56.3	−25.0
2	2.004	0.255	0.0193	77.7	9.4
3	1.990	0.259	0.0259	57.7	−21.9
4	2.023	0.250	0.0250	66.6	−5.8
5	1.938	0.272	0.0205	78.4	10.2
Average				67.3	−4.5
For GCr15 bearing steel					
Test no.	h_m (μm)	H_n (GPa)	W_e/W_t	E (GPa)	(E-204)/E (%)
1	1.924	7.156	0.288	219.0	6.9
2	1.942	7.026	0.288	213.8	4.6
3	1.939	7.048	0.282	219.7	7.1
4	1.962	6.880	0.283	212.4	4.0
5	1.936	7.063	0.288	215.6	5.4
Average				216.1	5.6
For fused silica					
Test no.	h_m (μm)	H_n (GPa)	W_e/W_t	E (GPa)	(E-72)/E (%)
1	1.997	4.632	0.667	73.4	1.9
2	1.999	4.623	0.664	73.4	1.9
3	1.997	4.633	0.664	73.6	2.2
4	1.996	4.635	0.661	73.7	2.4
5	1.996	4.634	0.666	73.4	2.0
Average				73.5	2.1

are given in Table II. It is seen that all the estimated values of Young's modulus for the three materials are close to the reference values. This validates once again the effectiveness of the proposed method.

V. CONCLUSIONS

In this study, we simulated indentation process performed on a homogeneous elastic–plastic solid with an elastic conical indenter by applying FEA, and reexamined the previously proposed H_n/E_r–W_e/W_t relationship. Results showed that E_r used in the relationship cannot accurately reflect the combined elastic effect of an indenter and an indented material, because the Young's modulus ratio $\eta = [E/(1 - \nu^2)]/[E_i/(1 - \nu_i^2)]$ can affect independently the dependence of H_n/E_r on W_e/W_t. Through defining a combined Young's modulus $E_c \equiv 1/[(1 - \nu^2)/E + 1.32(1 - \nu_i^2)/E_i] = E_r/[1 + 0.32\eta/(1 + \eta)]$ and using it to replace E_r, an effective one-to-one correspondence between H_n/E_c and W_e/W_t was established, which is found to be independent on η over a broad range from 0 to 0.3834. From this relationship, an improved method for estimating the Young's modulus of an indented material based on a microindentation test is proposed. The effectiveness of the method was verified by referring to some published microindentation data for two aluminum alloys 6061-T6511 and 7075-T651, and by the results of microindentation tests performed on three standard materials, i.e., aluminum single crystal, GCr15 bearing steel, and fused silica.

ACKNOWLEDGMENT

This work was supported by the National Natural Science Foundation of China (Grant No. 10672185).

REFERENCES

1. J.B. Pethica, R. Hutchings, and W.C. Oliver: Hardness measurement at penetration depth as small as 20 nm. *Philos. Mag. A* **48,** 593 (1983).
2. J.L. Loubet, J.M. Georges, O. Marchesini, and G. Meille: Vickers indentation curves of magnesium oxide (MgO). *J. Tribol.* **106,** 43 (1984).
3. D. Newey, M.A. Wilkens, and H.M. Pollock: An ultra-low-load penetration hardness tester. *J. Phys. E: Sci. Instrum.* **15,** 119 (1982).
4. W.C. Oliver and G.M. Pharr: An improved technique for determining hardness and elastic modulus using load and displacement sensing indentation experiments. *J. Mater. Res.* **7,** 1564 (1992).
5. G.M. Pharr, W.C. Oliver, and F.R. Brotzen: On the generality of the relationship among contact stiffness, contact area, and elastic modulus during indentation. *J. Mater. Res.* **7,** 613 (1992).
6. W.C. Oliver and G.M. Pharr: Measurement of hardness and elastic modulus by instrumented indentation: Advances in understanding and refinements to methodology. *J. Mater. Res.* **19,** 3 (2004).
7. Y-T. Cheng and C-M. Cheng: Relationships between hardness, elastic modulus, and the work of indentation. *Appl. Phys. Lett.* **73,** 614 (1998).
8. Y-T. Cheng and C.M. Cheng: Scaling, dimension analysis, and indentation measurements. *Mater. Sci. Eng., R* **44,** 91 (2004).
9. D. Ma, C.W. Ong, and T. Zhang: An improved energy method for determining Young's modulus by instrumented indentation using a Berkovich tip. *J. Mater. Res.* **23,** 2106 (2008).
10. D. Ma, C.W. Ong, and T. Zhang: An instrumented indentation method for Young's modulus measurement with accuracy estimation. *Exp. Mech.* **49,** 719 (2009).
11. M. Dao, N. Chollacoop, K.J. Van Vliet, T.A. Venkatesh, and S. Suresh: Computational modeling of the forward and reverse problems in instrumented sharp indentation. *Acta Mater.* **49,** 3899 (2001).
12. M. Lichinchi, C. Lenardi, J. Haupt, and R. Vitali: Simulation of Berkovich nanoindentation experiments on thin films using finite element method. *Thin Solid Films* **312,** 240 (1998).
13. A.C. Fischer-Cripps: Use of combined elastic modulus in depth-sensing indentation with a conical indenter. *J. Mater. Res.* **18,** 1043 (2003).
14. ABAQUS: version 6.2 (Hibbitt, Karlsson & Sorensen, Inc., Pawtucket, RI, 2001).
15. H. Lan and T.A. Venkatesh: Determination of the elastic and plastic properties of materials through instrumented indentation with reduced sensitivity. *Acta Mater.* **55,** 2025 (2007).
16. L. Liu, N. Ogasawara, N. Chiba, and X. Chen: Can indentation technique measure unique elastoplastic properties? *J. Mater. Res.* **24,** 784 (2009).